Single beam interferometric angle measurement

Pierdomenico Paolino, Ludovic Bellon

Single beam interferometric angle measurement

P. Paolino, L. Bellon
École Normale Supérieure de Lyon, Laboratoire de Physique
C.N.R.S. UMR5672
46, Allée d'Italie, 69364 Lyon Cedex 07, France

December 12, 2006

Abstract

We present a new application of the Nomarski interferometer, to measure the angular position of a parallel laser beam with interferometric precision. In our experimental realization we reach a resolution of 3×10^{-9} rad (6×10^{-4} ″) for 1 kHz bandwidth in a 2×10^{-2} rad (1°) range. This alternative to the optical lever technique features absolute calibration, independence of the sensitivity on the thermal drifts, and wide range of measurement at full accuracy.

PACS: 07.60.Ly, 06.30.Bp

1 Introduction

Angle measurement is important in a number of applications, ranging from machine tool operation to calibration of optical prism through atomic force microscopy detection. This basic metrological task can be performed in many ways with optical methods [1], using for instance an autocollimator [2], an interferometric setup (see for example [3]) or an optical lever scheme with an electronic target (such as a segmented photodiode) [4, 5]. A major challenge of these techniques is to allow both a wide range of measurement and a high precision simultaneously. We will focus here on interferometric setups, which are usually restricted to small angle measurements but feature very good accuracy. After a generic introduction to the sensitivity of these techniques, we will present how their range can be greatly expanded without losing in precision using a quadrature phase approach. This novel technique to perform calibrated measurements of the angular position of a parallel laser beam is based on a quadrature phase Normarski interferometer [6], except for the laser beam configuration: in the current setup, a single beam directly enters the calcite prism and the common part of two resulting beam is directly analyzed.

The paper is organized as follows: in section 2 we explain the principle of the technique under a wider approach of interferometric angle measurements, while in section 3 we describe the actual experimental realization and we report the results of the calibration measurements, emphasizing how this technique allows constant recording of tiny rotations independently from thermal drifts. In section 4 we discuss the sources of noise for the measurements. In section 5 we compare our technique to the widespread optical lever technique (based on a 2 quadrants photodiode's detection), before concluding in section 6.

2 Interferometric angle measurement: principle

Let us first discuss the general background of the measurement we want to perform here: we consider a single laser beam with origin O in the $\mathbf{e}_x, \mathbf{e}_y$ plane, and we would like to measure through interferometry its angular direction (the rotation is thus defined around $\mathbf{e}_z$). In the analyzing region, there should be at least 2 beams in order to have interference. To achieve

the best contrast possible, these two beams should have a constant phase difference over the sensor area. This implies in general (given that the sensor is flat and its size is much greater than the wavelength λ) that the 2 analyzing beams are parallel plane waves over the sensor, and thus in the free space just before it. Their common wave vector is denoted by $\mathbf{k}$ in this region (see Fig.1).

Let us now consider the optical path of a ray from the origin O of the incident beam to point A of the first analyzing beam, and a equivalent path from point O to B in the second beam, such that the optical lengths are equal: OA=OB. As long as A an B are chosen in the free space region before the sensor, the phase difference between the two beams is

$$\varphi = \mathbf{k}.\mathbf{AB}$$

If we make an infinitesimal change of the incident laser beam, A will change to $A' = A + \delta\mathbf{A}$ and B to $B' = B + \delta\mathbf{B}$, where we still impose that OA'=OA=OB'=OB. The corresponding phase variation between the two beams is thus

$$\delta\varphi = \delta\mathbf{k}.\mathbf{AB} + \mathbf{k}.\delta\mathbf{AB}$$

$$\delta\varphi = \delta\mathbf{k}.\mathbf{AB} + \mathbf{k}.\delta\mathbf{B} - \mathbf{k}.\delta\mathbf{A}$$

According to Fermat's principle, the optical path is extremal, which implies for free space propagation that the direction of propagation of light is perpendicular to the iso optical length surfaces. It translates here into $\mathbf{k}.\delta\mathbf{B} = \mathbf{k}.\delta\mathbf{A} = 0$, so that

$$\delta\varphi = \delta\mathbf{k}.\mathbf{AB}$$

Noting that $|\mathbf{k}| = 2\pi/\lambda$ is a constant, we will only sense rotation of the interfering beams with a sensitivity

$$\frac{\partial\varphi}{\partial\theta} = \frac{2\pi}{\lambda}d \tag{1}$$

where θ is the angular direction of the beams, and d their separation perpendicular to the propagation (see Fig.1).

The only assumption underlying the previous calculation is that the optical systems is still: Fermat's principle applies to a constant refractive medium. Let us add the hypothesis that the angular magnification is one, and we can apply eq. 1 to the dependence of the phase difference between the two interfering beams over the orientation of the incident beam.

According to eq. 1, it sounds like there is no limit to the sensitivity, as it is increasing linearly with the distance between the two light rays. However, one should keep in mind that the beams have a finite lateral extension, and to record interference we should overlap them. In gaussian beam approximation, one can show that the optimum sensitivity is achieved when the separation d is equal to the $1/e^2$ radius of the beams (see section 3, eq. 6).

3 Experimental setup

We present in this section the experimental setup we have built to demonstrate the workability of an interferometric measurement of the angular position of a single light beam, as schemed on fig. 2. The output of an He-Ne laser is sent into a single-mode polarization maintaining fiber, then collimated to a parallel beam of $1/e^2$ diameter $2W = 6.6\,\text{mm}$. The fiber end and collimator are hold by a kinematic mount with a piezo drive to change the angular direction θ of the light beam before it enters a 40 mm calcite prism. We end up with two parallel beams of crossed polarization, separated by $d = 4\,\text{mm}$, thus overlapping a few millimeters. A diaphragm limits the output to this overlapping area. The intensities of the 2 light rays are evenly tuned by adjusting the incident polarization at 45° with respect to the calcite optical axes. No interference can be seen at this stage since the two beams have crossed polarizations, though they present a phase shift φ dependent on the angle of incidence θ of the initial beam on the calcite.

To analyze these overlapping beams, we use a quadrature phase technique similar to the one of ref. [6]. They are first divided into two equivalents rays with a non polarizing cube beamsplitter. In both arms, the beam is focused on the detector through a second 5 mm calcite prism, which optical axis are oriented at 45° with respect to the first one. We project this way the two initial polarizations and make the two incident beams interfere: the intensities A and B of the 2 beams emerging the last calcite prism are functions of the phase shift φ and can be recorded by two photodiodes (since the two spots are only 0.5 mm distant, we actually use a 2 quadrants photodiode). In the second analyzing arm, a quarter wave plate is added in order to subtract $\pi/2$ to the phase shift φ between the two cross polarized beams.

Measured intensities A_n, B_n in the two analyzing arms n (with $n = 1, 2$)

are easily computed as:

$$\begin{aligned} A_n &= \frac{I_0}{4}(1 + C_{max}\cos(\varphi + \psi_n)) \\ B_n &= \frac{I_0}{4}(1 - C_{max}\cos(\varphi + \psi_n)) \end{aligned} \tag{2}$$

where I_0 is the total intensity corresponding to the incident light beam[1], C_{max} is a contrast factor which accounts for lateral extension of the beams ($C_{max} < 1$), and $\psi_1 = 0$ (first arm, without quarter wave plate) or $\psi_2 = -\pi/2$ (second arm, with quarter wave plate). With adapted low noise analog conditioning electronic, we can measure for each arm the contrast function of these two signals:

$$C_n = \frac{A_n - B_n}{A_n + B_n} = C_{max}\cos(\varphi + \psi_n) \tag{3}$$

This way, we get rid of fluctuations of laser intensity, and have a direct measurement of the cosine of the total phase shift for each arm, $\varphi + \psi_n$.

Let us rewrite eq. 3 as:

$$C = C_1 + i\,C_2 = C_{max}\,(\cos(\varphi) + i\sin(\varphi)) = C_{max}e^{i\varphi} \tag{4}$$

Under this formulation, the advantage of using two analyzing arms instead of one is obvious : it allows one to have a complete determination of φ (modulo 2π). In the (C_1, C_2) plane, a measurement will lie on the C_{max} radius circle, its polar angle being the phase shift φ. All we need to do is acquire the two contrasts and numerically compute φ. Eq. 1 can directly be used to compute the sensitivity of the measurement of the angular position of the incident beam[2]: all the hypothesis of section 2 are met (still optics, angular magnification one).

The sensitivity appears this way to be independent of the position on the circle of the measurement, and will be constant even with a slow thermal drift. The beam separation d is in reality function of the angle of incidence θ, but its variation is small in the full θ range available: the main limitation to the angle of incidence that can be measured is that each beam emerging the

[1] I_0 is the electrical intensity defined by $I_0 = SP$, where P is the incident beam power (in W) and S is the responsivity of the photodiodes (in A/W). The 1/4 factor in the equations accounts for the beam-splitting process (2 final beams in both analyzing arms).

[2] The same formula can be derived directly analyzing the particular design of the optical setup of fig. 2, using birefringence laws instead of the formalism of section 2.

last calcites in the analyzing arms should fall on its respective photodiode quadrant. Given the focal length of the focusing lens ($f = 25\,\mathrm{mm}$) and the separation of the 2 beams ($d' = 0.5\,\mathrm{mm}$), the range accessible in θ in our setup is $\theta_{max} = d'/f = 2 \times 10^{-2}\,\mathrm{rad}$. Note that this range can be greatly extended if useful, choosing a larger separation of the final beams (using a Wollaston prism and 2 distinct photodiodes for example [7]).

To demonstrate the operation of this technique, we rotate the beam by means of a piezoelectric ceramic. The driving voltage that we use is the sum of two sinusoids: a fast one of low amplitude (leading to a μrad rotation) and a slow one of high amplitude (simulating a slow drift of the working point of the interferometer over several wavelengths, that is a rotation of about 1 mrad). In Fig. 3(a), we plot as a function of time a typical driving of the beam's angular rotation θ. In this specific case the slow and fast sinusoids have a frequency of 10 mHz and of 10 Hz respectively and the amplitude ratio is about 400. The contrasts C_1 and C_2 of the two analyzing arms, as expected, are in phase quadrature. In Fig. 4 we also plot the contrasts C_1 and C_2 in the (C_1, C_2) plane to show that they lay on a circle. In fact, the measurement lays on a tilted ellipse, but this deviation from the C_{max} radius circle can easily be corrected [8].

Let us now have a closer look at the fast evolution of these signals. In Fig. 5 we plot as a function of time the fast angular displacement $\delta\theta$ and contrasts c_n obtained by a high pass filtration of the signals θ and C_n. Comparing Figs. 5(b) and (c) with Figs. 3(b) and (c) we see that $c_1(c_2)$ goes to 0 periodically when $C_1(C_2)$ is extremal while the reconstructed angular position has a constant amplitude. Therefore this technique allows constant recording of small rotations as shown in the precedent paragraph. This is clearly seen in Fig. 6 where the fast evolution of $\delta\theta$, c_1 and c_2 are plotted on a time interval around a minimum of C_1 and C_2. The cleanness of the curve of Fig. 6(a) demonstrates the accuracy of this measurement.

4 Noise of the measurement

Let us compute the sensitivity σ of the contrast C as a function of the angle of incidence θ. Using eq. 1 and 4, we have:

$$\sigma = |\frac{\partial C}{\partial \theta}| = C_{max}\frac{2\pi}{\lambda}d \tag{5}$$

C_{max} can be computed analytically in the case of gaussian beams impinging a infinite size sensor. Let us for example consider intensity A_1:

$$A_1 \propto \iint dy\, dz\, |E_1 + E_2|^2$$

where

$$\begin{aligned} E_1 &= E_0 e^{-\frac{(y-d/2)^2+z^2}{W^2}} \\ E_2 &= E_0 e^{-\frac{(y+d/2)^2+z^2}{W^2}} e^{i\varphi} \end{aligned}$$

are the electric fields of each beam, and W is their $1/e^2$ radius. It is straightforward to show that

$$A_1 \propto \left(1 + e^{-\frac{d^2}{2W^2}} \cos(\varphi)\right)$$

and from eq. 2 we directly identify C_{max} as

$$C_{max} = e^{-\frac{d^2}{2W^2}} \tag{6}$$

The sensitivity σ being proportional to $C_{max}d$ (eq. 5), we can easily show that it is maximum when the separation between the beams is equal to their $1/e^2$ radius: $d = W$, where we get $C_{max} = 0.61$. In fact, this configuration is not the best one can use to maximize the sensitivity: adding a diaphragm to limit the beams to their common part, we can compute numerically the optimum parameters: $d/W = 1.08$ with a diaphragm of diameter $2.25W$, which lead to $C_{max} = 0.65$ and raise the sensitivity of 15%.

The main source of noise in the measurement is the unavoidable shot noise of the photodiodes. Let δA_n and δB_n be the intensity fluctuations on the photodiodes, their power spectra are white noises of spectral densities $S_{A_n} = 2eA_n$ and $S_{B_n} = 2eB_n$, e being the elementary charge. Moreover, these noises are uncorrelated. They will result in a fluctuation in the contrasts δC_n given by the equations:

$$\delta C_n = \delta \frac{A_n - B_n}{A_n + B_n} = 2\frac{B_n \delta A_n - A_n \delta B_n}{(A_n + B_n)^2}$$

The spectral density of noise of the contrast thus reads

$$S_{C_n} = 4\frac{B_n^2 S_{A_n} + A_n^2 S_{B_n}}{(A_n + B_n)^4} = 8e\frac{A_n B_n}{(A_n + B_n)^3}$$

Using eq. 2 and eq. 3, we have $A_n = I_0(1 + C_n)/4$ and $B_n = I_0(1 - C_n)/4$, hence

$$S_{C_n} = \frac{4e}{I_0}(1 - C_n^2)$$

Fluctuations in phase $\delta\varphi$ can be computed from eq. 4: $\delta\varphi = \delta C/iC$. Since φ is real, let us limit to its real part the second member of this equation to compute $\delta\varphi$:

$$\begin{aligned}
\delta\varphi &= Re\left(\frac{\delta C_1 + i\delta C_2}{iC_1 - C_2}\right) \\
&= \frac{C_1\delta C_2 - C_2\delta C_1}{C_1^2 + C_2^2} \\
S_\varphi &= \frac{C_1^2 S_{C_2} + C_2^2 S_{C_1}}{(C_1^2 + C_2^2)^2} \\
&= \frac{4e}{I_0}\frac{C_1^2(1 - C_2^2) + C_2^2(1 - C_1^2)}{(C_1^2 + C_2^2)^2} \\
&= \frac{4e}{I_0}\left(\frac{1}{C_{max}^2} - \frac{1}{2}sin^2(2\varphi)\right)
\end{aligned}$$

From this last equation, we eventually get an upper bound for the power spectrum density of shot noise induced fluctuations in θ:

$$S_\theta \leqslant \left(\frac{\lambda}{2\pi d}\right)^2 \frac{4e}{I_0}\frac{1}{C_{max}^2} = \frac{4e}{I_o\sigma^2} \tag{7}$$

In Fig. 8 we plot the power spectrum density S_θ produced by a still laser beam and the shot noise's estimation of our experiment. The pics in the $10\,\mathrm{Hz} - 10^3\,\mathrm{Hz}$ region are attributed to mechanical disturbances in the experimental setup and could be addressed by a quieter environment, while at low frequency (below 50 Hz) the electronics $1/f$ noise is visible. We can see that our setup is close to optimal conditions. Finally we note that in terms of optical path difference, these values correspond to a sensitivity of $2 \times 10^{-27}\,\mathrm{m}^2/\mathrm{Hz}$.

5 Comparison with optical lever technique

In the classic optical lever technique, the single beam illuminates a 2 quadrants photodiode, as sketched in fig. 7. A contrast function C_{2Q} of the

intensities of the two quadrants (ratio of the difference and the sum of the signals, similar to the one defined in eq. 3) can be used to measure the position of this light beam on the sensor. The output of a gaussian beam of $1/e^2$ radius w at a distance y of the zero width slit is:

$$C_{2Q} = \mathrm{erf}\left(\sqrt{2}\frac{y}{w}\right)$$

Where erf is the error function. The best sensitivity is obtained for $y \approx 0$ and for the smallest w, that is when the beam is focused on the sensor:

$$\left(\frac{dC_{2Q}}{dy}\right)_{y=0} = \frac{2\sqrt{2}}{\sqrt{\pi}w_0}$$

where w_0 is the radius of the beam waist. This spot is diffraction limited, so the size of the beam at its origin O can be computed by $W = \lambda l/\pi w_0$, where l is the distance between O and the sensor. When the beam direction changes of an angle $d\theta$, the position on the sensor is shifted by $dy = l d\theta$, and we eventually get

$$\begin{aligned} C_{2Q} &= \mathrm{erf}\left(\sqrt{2}\frac{\pi W}{\lambda}\theta\right) \\ \sigma_{2Q} &= \left(\frac{dC_{2Q}}{d\theta}\right)_{\theta=0} = \sqrt{8\pi}\frac{W}{\lambda} \end{aligned}$$

where the sensitivity σ_{2Q} is computed at $\theta = 0$. Given the shape of the erf function, the range of the measurement is inversely proportional to the sensitivity: $\theta^{2Q}_{max} \sim 1/\sigma_{2Q}$. For a 7 mm diameter laser beam at 633 nm, the admissible range is thus limited to 2×10^{-5} rad. This range can obviously be extended by degrading the sensitivity when defocusing the spot from the sensor.

A computation similar to the one of previous paragraph can be done to analyze the shot noise induced fluctuations in C_{2Q}, they result in a power spectral density $S_{C_{2Q}} = 2e/I_0$, which finally leads to

$$S^{2Q}_{\theta} = \left(\frac{\lambda}{W}\right)^2 \frac{1}{8\pi}\frac{2e}{I_0} = \frac{2e}{I_0\sigma^2_{2Q}} \tag{8}$$

We have supposed up to now a zero width slit for the segmented photodiode. Interestingly, the noise can be reduced by introducing a gap between the

quadrants [5]. The optimum value of the separation is $0.61 w_0$, which reduces the power spectrum density of shot noise induced fluctuations of 22%.

Using analytical expressions 7 and 8, the ratio of the noise of the two techniques eventually reads

$$\frac{S_\theta}{S_\theta^{2Q}} \leqslant 2\left(\frac{\sigma_{2Q}}{\sigma}\right)^2 = \left(\frac{W}{d}\right)^2 \frac{4}{\pi}\left(\frac{1}{C_{max}^2}\right)$$

Under optimal condition for both techniques, the numerical value of this ratio is 3.2, which means that the interferometric technique is a bit noisier than the optical lever technique, when both are perfectly tuned. Nevertheless, our setup offers key advantages over the 2 quadrants detection:

- *Absolute calibration*: the interferometric measurement only depends on λ and d, two quantities that can be precisely measured independently, whereas the optical lever sensitivity depends on the exact focalization of the beam and needs to be calibrated for every experiment.

- *Extended deflection range*: in the present example, deflection up to 10^3 greater can be studied with the interferometric method (and this factor could even be raised by choosing a bigger separation of the analyzing beams in each arms). It implies that strong variations of θ cannot be studied with great precision with the optical lever detection, for which any slow drift requires a constant adjustment of the 0. The sensitivity of our technique is moreover constant on the whole range.

- *Translation insensitive*: the measurement is only sensitive to the rotation we are probing (around $\mathbf{e}_z$), and is insensitive to any translation, whereas the other method will sense translation along $\mathbf{e}_y$ as well as rotation. Our technique is thus more selective and less sensitive to mechanical vibrations of the setup.

6 Conclusion

We have proposed an interferometric technique to measure the angular position of a laser beam, which can represent an alternative to the optical lever one. The sensitivity of this experimental realization is 3 nrad ($6 \times 10^{-4}\,''$) for 1 kHz bandwidth on a range of 20 mrad (1.15°), and it can be improved in

various ways (larger calcite and beam size, brighter light source, larger separation of beams in detection area, etc.) Although the sensitivity of the optical lever may be a bit better than that of the interferometric setup, our technique offers several advantages: robustness (insensitivity to thermal drift, and in general to mechanical vibrations expect for the rotation probed), absolute calibration, large angular range.

As a final remark, let us point out another way to use the setup: one can rotate the first calcite prism with a still laser beam. In this configuration, the sensitivity is unchanged and still described by eq. 1 (where θ stand for the angular position of the prism this time), but the range is greatly extended. The limitation is no longer due to the analyzing arms (the focusing lenses will always ensure that the beams fall on their respective photodiodes), but simply to the field of view of the initial calcite. For our setup, a 0.2 rad range can be easily be explored. Nevertheless, one should take into account variations of d with θ in this case, since they are not negligible over such a wide range of measurement.

Acknowledgements

We thank F. Vittoz and F. Ropars for technical support, and N. Garnier, S. Joubaud, S. Ciliberto and A. Petrosyan for stimulating discussions.

References

[1] D. Malacara, A. Cornejo, and M. V. R. K. Murthy. Bibliography of various optical testing methods. *Applied Optics*, 14(5):1065–1080, 1975. Section XIV.

[2] W. G. Driscoll, editor. *Handbook of Optics*. McGraw-Hill, New York, 1978.

[3] D. Malacara and O. Harris. Interferometric measurement of angles. *Applied Optics*, 9(7):1630–1633, 1970.

[4] R. V. Jones. Some developments and applications of the optical lever. *Journal of Scientific Instruments*, 38(2):37–45, 1961.

[5] M. G. L. Gustafsson and J. Clarke. Scanning force microscope springs optimized for optical-beam deflection and with tips made by controlled fracture. *J. Appl. Phys.*, 76(1):172–181, 1994.

[6] L. Bellon, S. Ciliberto, H. Boubaker, and L. Guyon. Differential interferometry with a complex contrast. *Opt. Commun.*, 207:49–56, 2002.

[7] C. Schonenberger and S. F. Alvarado. A differential interferometer for force microscopy. *Review of Scientific Instruments*, 60(10):3131–3134, 1989.

[8] P. L. M. Heydemann. Determination and correction of quadrature fringe measurement errors in interferometers. *Applied Optics*, 20(19):3382–3384, 1981.

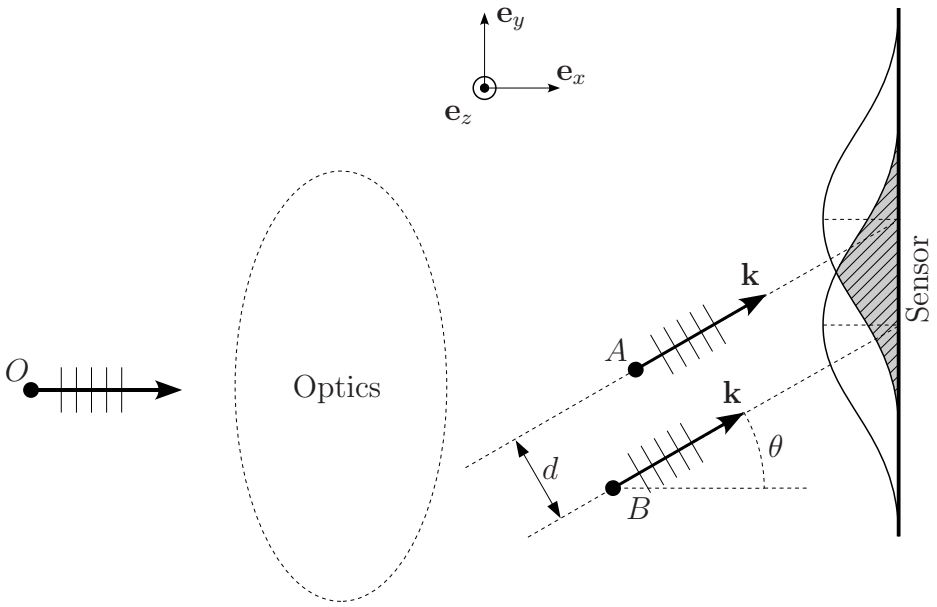

Figure 1: Principle of the single beam interferometric angle measurement: the incident light wave is split into two parallel beams in the analyzing region, where they interfere over the sensor.

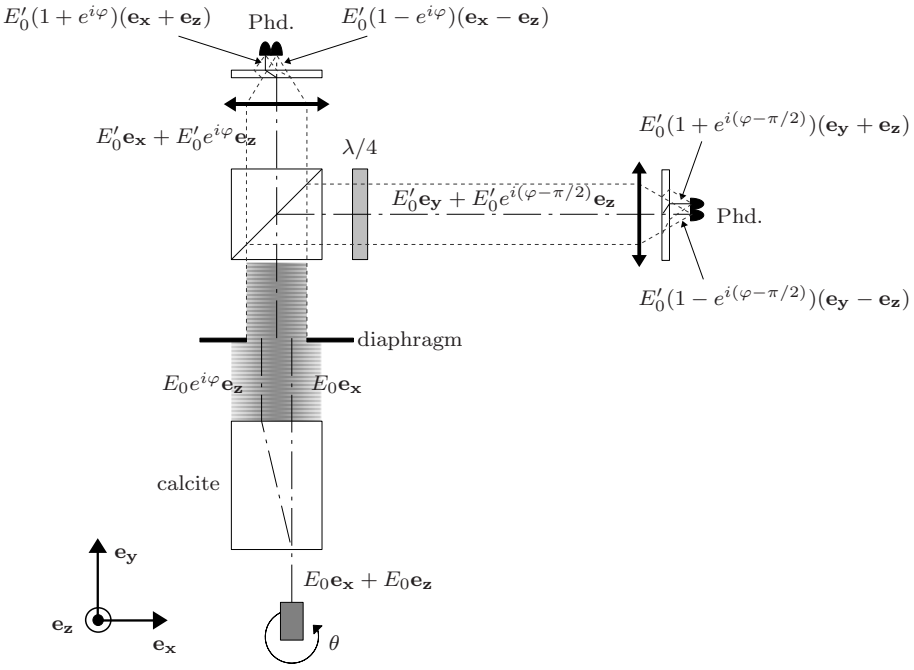

Figure 2: Experimental setup: a 6.6 mm collimated He-Ne laser beam can be rotated around $\mathbf{e}_z$ by means of a piezo driven kinematic mount. After passing through a 40 mm calcite prism, the 2 resulting crossed polarized rays present a phase shift φ dependent on the angle of incidence θ. We limit the 2 beams to their overlapping part using a diaphragm, and analyze them into two arms: a second calcite prism (5 mm thick) oriented at 45° with respect to the first one projects the polarizations and makes the beams interfere. In the second analyzing arm, a quarter wave plate is added in order to subtract $\pi/2$ to the phase shift φ. The beams are focused on 2 quadrants photodiodes to record their intensities, which are used to reconstruct φ and thus measure θ.

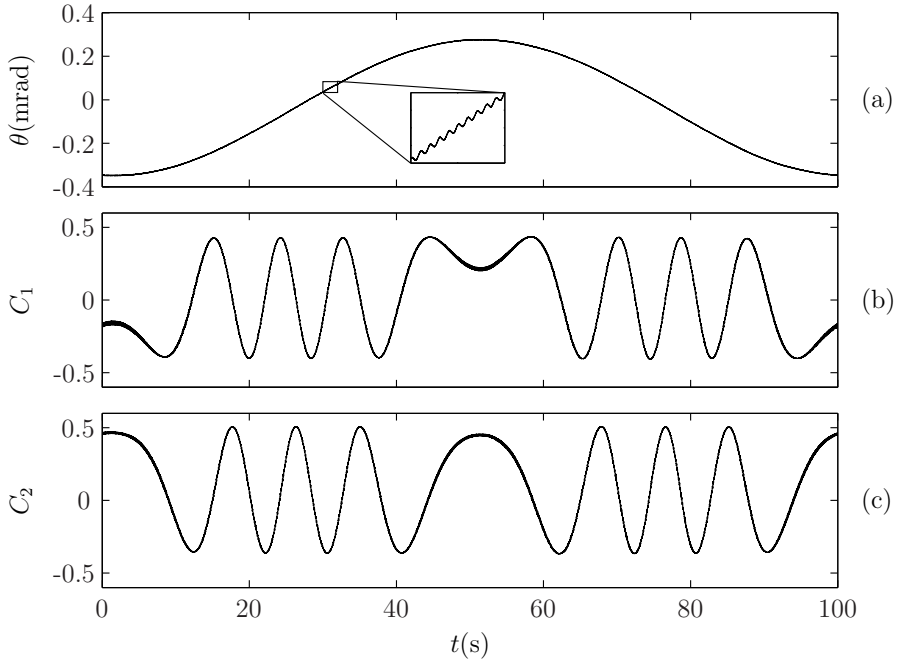

Figure 3: (a) Angular position θ of the laser beam. The driving is the sum of two sinusoids : 0.5 mrad at 10 mHz and 1 μrad at 10 Hz. (b) and (c) resulting contrasts C_1 and C_2 of the two analyzing arms as a function of time.

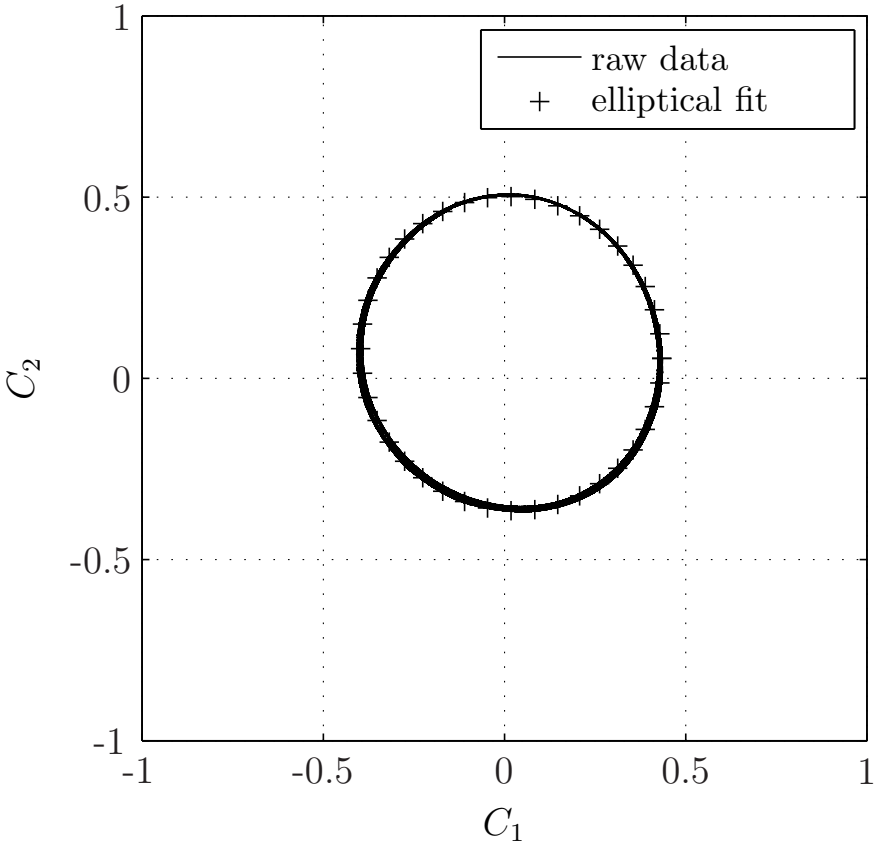

Figure 4: Due to experimental imprecisions, the measurement lays on a tilted ellipse in the C_1, C_2 plane. These deviations to the C_{max} radius circle can easily be corrected [8]. We present the raw data to show anyway that corrections are small.

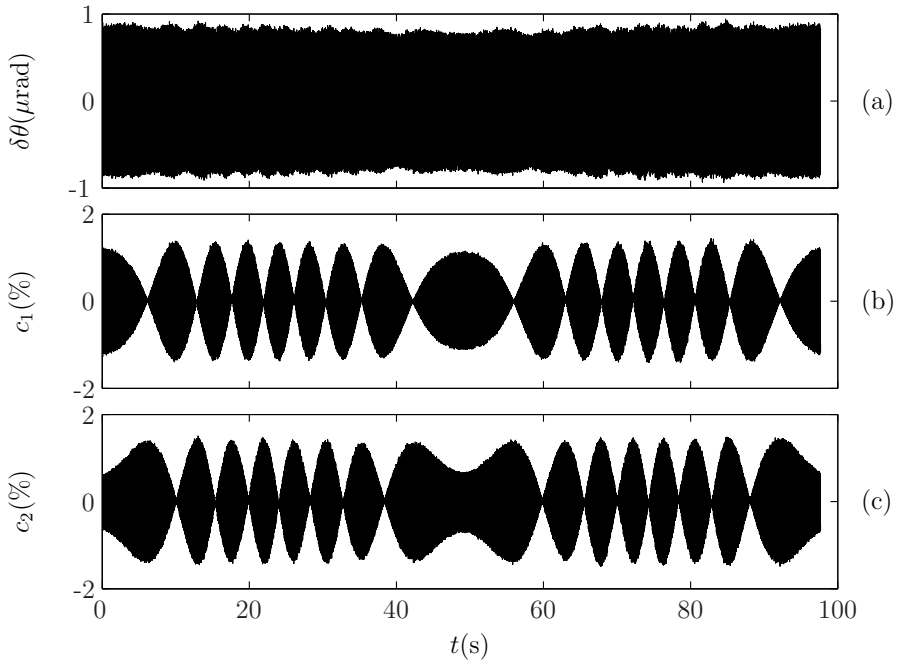

Figure 5: Fast evolution of the beam's angular position once the slow variation of Fig. 3 has been subtracted. (a) Fast angular displacement $\delta\theta$ as function of the time. (b) and (c) Fast contrasts c_i of the two analyzing arms.

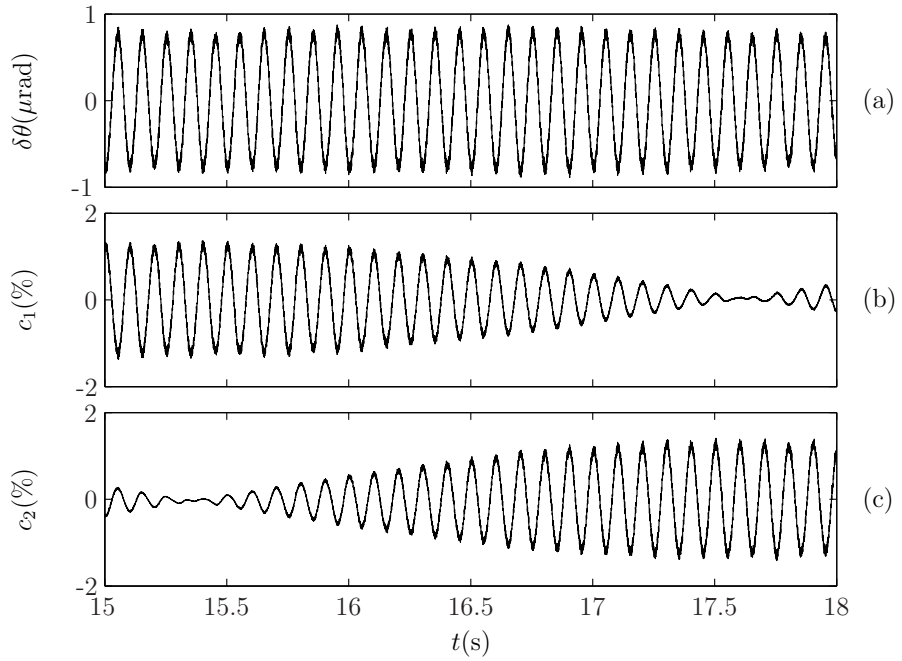

Figure 6: Zoom of Fig. 5: fast signals $\delta\theta$ (a), c_1 (b), c_2 (c) around minimums of C_1 and C_2. The reconstructed angular position $\delta\theta$ is independent of the working point.

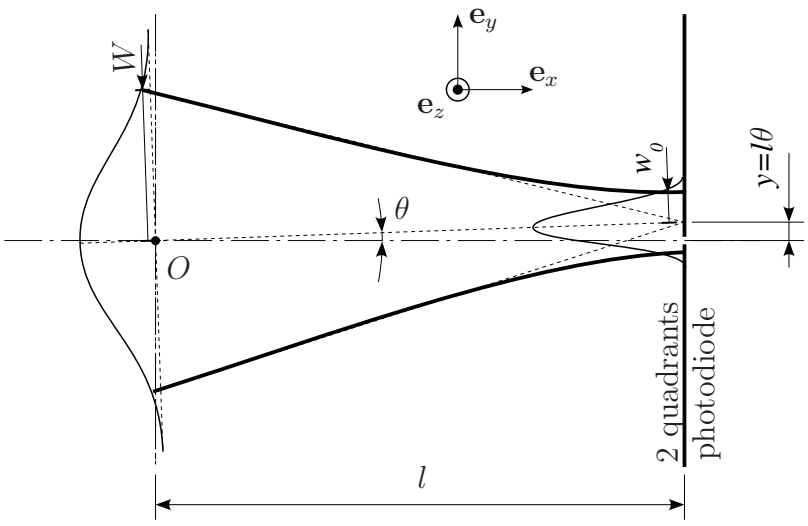

Figure 7: Principle of the optical lever technique: the incident beam is focused on a 2 quadrants photodiode, and for small deflections θ, the difference between the intensities on the 2 segments is a linear function of θ.

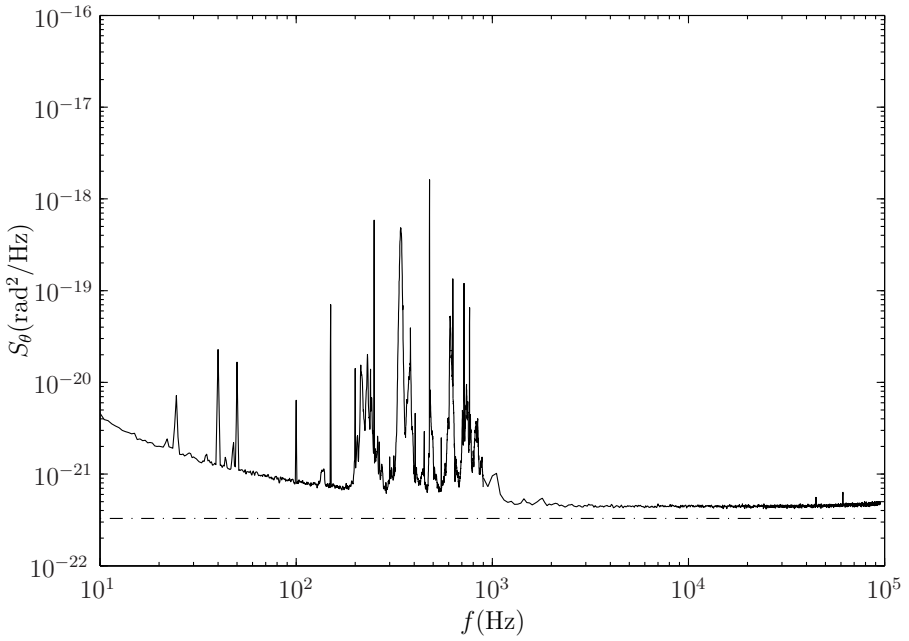

Figure 8: Power spectrum density of the angular deflection θ (plain line), and shot noise calculated from inequality 7 with experimental values of intensity and sensitivity (dash dotted line). The pics in the $10\,\mathrm{Hz} - 10^3\,\mathrm{Hz}$ region are attributed to mechanical disturbances in the experimental setup and could be addressed by a quieter environment. The integrated noise in the $0\,\mathrm{Hz} - 1\,\mathrm{kHz}$ range is 3 nrad, which is thus the lower limit of measurable angular displacement for this bandwidth.